Journal of
Nanomedicine & Nanotechnology

Rodrigues et al., J Nanomed Nanotechnol 2015, 6:3
DOI: 10.4172/2157-7439.1000286

Research Article Open Access

Photodynamic Therapy Based on Arrabidaea chica (Crajiru) Extract Nanoemulsion: *In vitro* Activity against Monolayers and Spheroids of Human Mammary Adenocarcinoma MCF-7 Cells

Mosar C Rodrigues[1], Luis A Muehlmann[2], João PF Longo[1], Renata C Silva[1], Ilmar B Graebner[3], Igor A Degterev[3,4], Carolina M Lucci[1], Ricardo B Azevedo[1] and Mônica P Garcia[1*]

[1]*Department of Genetics and Morphology, Institute of Biological Sciences, University of Brasilia, Federal District, Brazil*
[2]*Faculty of Ceilandia, University of Brasilia, Federal District, Brazil*
[3]*Center of Biologic and Natural Sciences, Federal University of Acre, Rio Branco, Acre, Brasil*
[4]*Institute of Chemistry and Biology, I. Kant Federal University, Kaliningrad, Russia*

Abstract

Natural products have been sources of numerous drugs over the history. However, little is known about the therapeutic potential of Amazon forest species. This work aimed at testing the potential of the hydrophobic extract of *Arrabidaea chica* (ACE), an Amazon plant, as a source of photosensitizers for anticancer photodynamic therapy. ACE was tested as a nanoemulsion (ACE-NE) produced by phase inversion temperature. It was found that ACE-NE intensely absorbs red light and, under photoactivation (λ 660 nm, 4.5 J/cm^2), produces reactive oxygen species. Photoactivated ACE-NE presented, *in vitro*, a CC_{50} of 1.3 µg ACE/mL against human breast adenocarcinoma MCF-7 cells, and was effective in lysing MCF-7 spheroids. In the dark, ACE was toxic neither to human mammary epithelial MCF-10A cells nor to MCF-7 cells. On that ground, this work is the first to show that *A. chica* is a source of photosensitizers potentially useful for anticancer photodynamic therapy.

Keywords: Spontaneous emulsification; Cancer; Amazon natural extracts; Human breast adenocarcinoma MCF-7 cells; Spheroids

Introduction

Despite the great advances reached in the design and synthesis of new drugs, natural products remain the main source of new therapeutic molecules [1]. It is remarkable, in this context, that Amazon forest, despite being one of the most species-rich biome in the planet [2], is still poorly studied for the therapeutic potential of its plants. This work investigates the photodynamic activity of an Amazon plant, *Arrabidaea chica* (Verlot; Bignoniaceae, popularly known as Crajiru, Carajuru, Puca Panga, Chica or Pariri), against cancerous cells *in vitro*. To the authors' knowledge, the photodynamic activity of *A. chica* was not studied by other research groups.

Photodynamic therapy (PDT) is approved by different agencies for the treatment of cancer [3-6]. It is based on three separately innocuous components, ground-state triplet oxygen ($^3O_2$), photosensitizer (PS), and light, which are extremely toxic to biological cells once combined. When the PS is irradiated by light at specific wavelengths, it becomes activated and converts triplet oxygen ($^3O_2$) into singlet oxygen ($^1O_2$), which is a strong oxidant and elicit oxidative stress if generated at sufficient amounts in a target cell, such as a cancerous cell [7-9]. This may lead to cell death or stress of therapeutic significance [10,11]. Intense efforts have been done in the search for new PS molecules, a single molecule presenting all the properties of an ideal PS for PDT is not known [5,7]. PS molecules are generally dyes that intensely absorb light at the red-near infrared region of the electromagnetic spectrum [8]. *A. chica* presents different polyphenolic and other compounds [12] that may, in principle, act as PS. Thus, this work aimed at investigating the potential of *A. chica* as a source of PS molecules.

Experimental

Materials

The reagents employed in this work are as follows: Dulbecco's modified Eagle's medium (DMEM, HyClone, Logan, USA); DMEM:F12 (HyClone, Logan, USA); penicillin, streptomycin and fetal bovine serum (Gibco, Grand Island, NY, USA); capric/caprilyc triacylglycerides (Polytechno, São Paulo, SP, Brazil); phosphate-buffered saline (Laborclin, Pinhais, Paraná, Brazil); dimethyl sulfoxide and ethanol (Vetec, Xerém, Rio de Janeiro, Brazil). Cell lines: human mammary adenocarcinoma MCF-7 cells (Rio de Janeiro Cell Bank [RJCB], Rio de Janeiro, Brazil), and human mammary epithelial MCF-10A cells (kindly provided by Dr. Maria Mitzi Brentani, University of São Paulo, São Paulo, Brazil). All other materials were purchased from Sigma (São Paulo, Brazil).

Preparation of *Arabidea chica* extract

Aerial parts of *A. chica* were collected on January 2011, at Florestal Humaitá Reserve (9°45'18"S 67°36'50"W), 33 km from Rio Branco, Acre/Brazil. The aerial parts were first dried in an oven at 50°C for 24 h. Exactly 4,650 g of aerial parts yielded 2,300 g of dried material. Eight hundred grams of this dried material were manually crushed and put into ethanol 98° GL for 24 h. The ethanol solution was then filtered and evaporated under reduced pressure in the rotaevaporator. The recovered ethanol was reused for further extraction on the same plant material, and this process was repeated until no staining was observed in the liquid. This extraction yielded 68 g of dried ethanol extract. Then, 68 g ethanol extract were infused in 200 mL chloroform. The solid-

***Corresponding author:** Mônica P Garcia, Department of Genetics and Morphology, Institute of Biological Sciences, University of Brasilia, Federal District, Brazil, Tel: 55-61 3307-2169; E-mail: mgarcia@unb.br

Received February 27, 2015; **Accepted** April 11, 2015; **Published** April 20, 2015

Citation: Rodrigues MC, Muehlmann LA, Longo JPF, Silva RC, Graebner IB, et al. (2015) Photodynamic Therapy Based on *Arrabidaea chica* (Crajiru) Extract Nanoemulsion: *In vitro* Activity against Monolayers and Spheroids of Human Mammary Adenocarcinoma MCF-7 Cells. J Nanomed Nanotechnol 6: 286. doi:10.4172/2157-7439.1000286

free chloroform extract was then dried at reduced pressure, yielding 1.8 g of dried chloroform *A. chica* extract (ACE), which was used for experiments described in this work.

Production of nanoemulsions containing chloroform extract of *Arrabidaea chica*

Cremophor ELP® (polyoxyl-35 castor oil) was used as surfactant and capric/caprylic triacylglycerides (CCT) as the oil phase. The nanoemulsion was produced by a phase inversion temperature (PIT) method [13]. Briefly, 3 g CCT and 9 g Cremophor ELP® were mixed under magnetic stirring at 45°C, and 350 mg ACE were added. After 30 minutes of mild stirring the solution became homogenous, and 20 g distilled water at room temperature were then added. A coarse, opaque emulsion formed. Then, the mixture was heat up to 95°C, 20 g distilled water at 4°C were added, and the mixture was cooled down in an ice bath. The volume was finally set to 50 mL with distilled water. A translucent, dark yellowish green nanoemulsion was obtained, which was stored in the dark at 4°C until usage. This ACE-containing nanoemulsion is referred to as ACE-NE along the text. Blank nanoemulsions (BL-NE), without ACE, were produced by the same procedure.

Colloidal properties

Before measurements, ACE-NE was diluted to 140 µg ACE/mL with distilled water, DMEM or DMEM:F12. Hydrodynamic diameter and zeta potential of nanodroplets of nanoemulsions were measured at 25°C by photon correlation spectroscopy and electrophoretic laser Doppler velocimetry (ZetaSizer Nano ZS®, Malvern Instruments, Malvern, UK), respectively. Polydispersity index (PDI) was estimated from DLS measurements by the equipment software. Measurements were performed in triplicates.

Photophysical properties

Fluorescence intensity and light absorption were measured with a spectrophotometer (Spectramax® M2, Molecular Devices, Sunnyvale, CA, USA), at 25°C, in 96-well microplates. In all experiments, ACE-NE was diluted with distilled water to 140 µg/mL before measuments.

Detection of reactive oxygen species

Reactive oxygen species (ROS) were detected with the probe 1,3-diphenylisobenzofuran (DPBF) [14,15]. Briefly, ACE-NE was diluted in water to concentrations ranging from 0.3 to 100.0 ng/mL. Then, 10 µL of DPBF (225 µg/mL in ethanol) were added to 200 µL of each sample in a transparent 96-well microplate. Next, absorption at λ 410 nm was measured at 25°C with a spectrophotometer, before and after irradiation of samples with light-emitting diode (LED, λ 660 nm), with light energy densities ranging from 0.1 to 4.5 J/cm^2. The same procedure was performed with pure BL-NE. The optical density at λ 410 nm before irradiation was considered as 0% ROS production, while the lower plateau absorption values were considered as 100% ROS production. Results were expressed as ROS production (%) in function of energy density. This experiment was performed in triplicate.

Cell culture

MCF-7 cells were cultured in Dulbecco's modified Eagle's medium (DMEM), supplemented with 10% (v:v) fetal bovine serum and 1% (v:v) antibiotic solution (100 IU/mL penicillin and 100 mg/mL streptomycin). MCF-10A cells were cultured in DMEM/F12 (1/1, v:v) supplemented with 5% (v:v) equine serum, 20 ng/mL epidermal growth factor (EGF), 10 µg/mL bovine insulin, 0.5 µg/mL hydrocortisone, 100 ng/mL cholera toxin, and 1% (v:v) antibiotic solution (100 IU/mL penicillin and 100 mg/mL streptomycin). All cells were maintained at 37°C in a 5% CO_2 humidified atmosphere.

Subcellular distribution of ACE-NE

The subcellular localization of ACE was visualized by confocal microscopy. Briefly, MCF-7 cells were cultured on coverslips placed in 12-well plates for 24 h, accordingly to conditions described in "Cell culture", at a density of 5×10^4 cells/well. Next, cells were exposed to ACE-NE diluted in culture medium, at a concentration equivalent to 125 µg ACE/mL, for 15 minutes, at 37°C, 5% CO_2 and humidified atmosphere. Then, cells were washed twice with PBS, stained with 4',6-diamidino-2-phenylindole (DAPI) for 15 minutes at room temperature, fixed with paraformaldehyde 4% (w:v) for 30 minutes, washed twice with PBS, and mounted on glass slides. Next, cells were visualized in confocal microscope (Leica, TCS SP5, São Paulo, Brazil). DAPI fluorescence was detected with excitation λ 358 nm and emission λ 461 nm. ACE fluorescence was detected with excitation λ 358 nm and emission λ 690 nm.

Formation of MCF-7 cells spheroids

Spheroids were obtained as described elsewhere [16]. Briefly, 50 µL low melting agarose 1.5% (w:v in distilled water) were added to wells of a 96-well microplate. Next, 1.5×10^4 MCF-7 cells processed as described in "Cell culture" were seeded on each well. The microplate was then centrifuged for 15 minutes at 1,500×g. Next, cells were kept at 37°C in a 5% CO_2 humidified atmosphere until spheroids of ca 200 µm in diameter were obtained (about 6 days). Each well contained one single spheroid. Next, spheroids were treated as described in "Cells treatment design" section.

Cells treatment design

MCF-7 and MCF-10A cells maintained as described in "Cell culture" and received one of the following treatments: 1) only culture medium; 2) irradiation with LED light (λ 660 nm) at energy density of 4.5 J/cm^2; 3) exposure to BL-NE dispersed in culture medium, for 15 minutes in the dark, at concentrations of nanodroplets (Cremophor ELP® plus CCT) of 17.1, 34.3 and 51.4 mg/mL – equivalent to 0.5, 1.0 and 1.5 mg ACE/mL if compared to ACE-NE; 4) exposure to BL-NE dispersed in culture medium, for 15 minutes in the dark, at concentrations of nanodroplets (Cremophor ELP® plus CCT) of 17.1, 34.3 and 51.4 mg/mL, and then irradiation with LED light (λ 660 nm) at energy density of 4.5 J/cm^2, **5)** exposure to ACE-NE diluted in culture medium, for 15 minutes in the dark, at concentrations ranging from 0.02 to 1,000.00 µg ACE/mL, **6)** exposure to ACE-NE diluted in culture medium, for 15 minutes in the dark, at concentrations ranging from 0.02 to 1,000.00 µg ACE/mL, washed twice with PBS, and then irradiation with LED light (λ 660 nm) at energy density of 4.5 J/cm^2. Next, cells were cultured for 24 h accordingly to the protocol described in "Cell culture", and their viability was then assessed by the MTT assay, as described in "MTT method for cell viability assessment".

MCF-7 cells spheroids were exposed for 30 or 60 minutes to PBS (no ACE control), or to ACE-NE at concentrations of 60.0, 110.0 or 230.0 µg ACE/mL. For each treatment, one half of wells containing spheroids was kept in the dark, while the other half was irradiated with LED light (λ 660 nm) at energy density of 4.5 J/cm^2. Immediately after the treatments, the viability of cells was assessed by the quantification of lactate dehydrogenase activity in culture supernatant, as described in "Measurement of lactate dehydrogenase activity".

MTT method for cell viability assessment

Viability of cells in monolayers was assessed by the method of 3,4,5-dimethylthiazol-2,5 biphenyl tetrazolium bromide (MTT) [17]. In

a typical experiment, cells were washed twice with PBS after receiving their respective treatment, and then incubated with 0.5 mg MTT/mL in culture medium for 2.5 h at 37°C, 5% CO_2 and humidified atmosphere. Then, cells were washed with PBS, and formazan was extracted from cells with 200 µL DMSO. The light absorption was then measured at λ 595 nm with a spectrophotometer (Spectramax M2, Molecular Devices, USA). This experiment was performed in quintuplicate for each treatment and the results were expressed as percentages relative to control (treated with PBS alone).

Measurement of lactate dehydrogenase activity

Lysis of cells in spheroids was assessed by the quantification of lactate dehydrogenase activity in culture supernatant by a colorimetric assay (CytoTox 96®, Promega Corp., Madison, WI, USA). Briefly, 40 µL of spheroid culture were mixed with 40 µL of CytoTox 96® and maintained in the dark for 30 minutes. Next, light absorption was read at λ 490 nm. Results were expressed as arbitrary units (au) of lactate dehydrogenase activity.

Statistical analyses

All statistical analyses were performed with GraphPad Prism 5.0 software. Statistical differences between groups were assessed by one-way analysis of variance (ANOVA), followed by Bonferroni's posttest (α=0.05). Results are expressed as mean of replicates ± SEM (standard error of the mean).

Results

Colloidal and photophysical properties of ACE-NE

As ACE is insoluble in aqueous media, it was nanoemulsified before measurements of photophysical properties and tests with cells. Table 1 presents the colloidal properties of ACE-NE in water, DMEM and DMEM:F12, and BL-NE in water. HD, PDI and Zeta potential were not affected by the type of dispersant tested. ACE-NE presented HD about 29 nm, with a low PDI, showing to be monodisperse. The Zeta potential was only slightly negative, reflecting the neutral characteristic of Cremophor ELP®, the surfactant used in this work.

ACE-NE presented a peak of fluorescence emission at λ 672 nm when excited with light of λ 400 nm (Figure 1A). Noteworthy, it intensely absorbs light at λ 668 nm (Figure 1B). As expected, BL-NE did not presented peaks of light absorption, only a slight turbidity revealed by its optical density all over the spectrum. Fluorescence of BL-NE was also negligible.

Production of reactive oxygen species

ACE-NE produced ROS in an ACE concentration- and light energy density-dependent fashion (Figure 2). The maximum production was reached with 30.0 and 50.0 ng/mL at the energy densities of 4.5 and 3.2 J/cm², respectively. As expected, BL-NE did not produce ROS when irradiated.

PDT mediated by ACE-NE in monolayers of MCF-7 and MCF-10A cells in vitro

BL-NE, in the dark or irradiated, at concentrations of 17.1, 34.3 and 51.4 mg/mL – equivalent to 0.5, 1.0 and 1.5 mg ACE/mL if compared to ACE-NE –, was not significantly toxic to both MCF-7 and MCF-10A cells (data not shown). Moreover, LED light alone, at the energy density of 4.5 J/cm², did not affect MCF-7 and MCF-10A cells viability (data not shown).

In the dark, it was not observed any significant trend of reduction in viability of both MCF-7 and MCF-10A by ACE-NE in the range of

Nanoemulsion/ Dispersant	HD (nm)	PDI	Zeta potential (mV)
ACE-NE/water	29.56 ± 0.63	0.140 ± 0,01	- 3.43 ± 0.23
ACE-NE/DMEM	29.45 ± 5.54	0.189 ± 0.01	- 3.57 ± 0.82
ACE-NE/DMEM:F12	28.78 ± 3.45	0.179 ± 0.02	- 3.45 ± 0.78
BL-NE/water	27.45 ± 0.54	0.090 ± 0.02	- 4.56 ± 0.32

Table 1: Colloidal properties of ACE-NE and BL-NE in different dispersants.

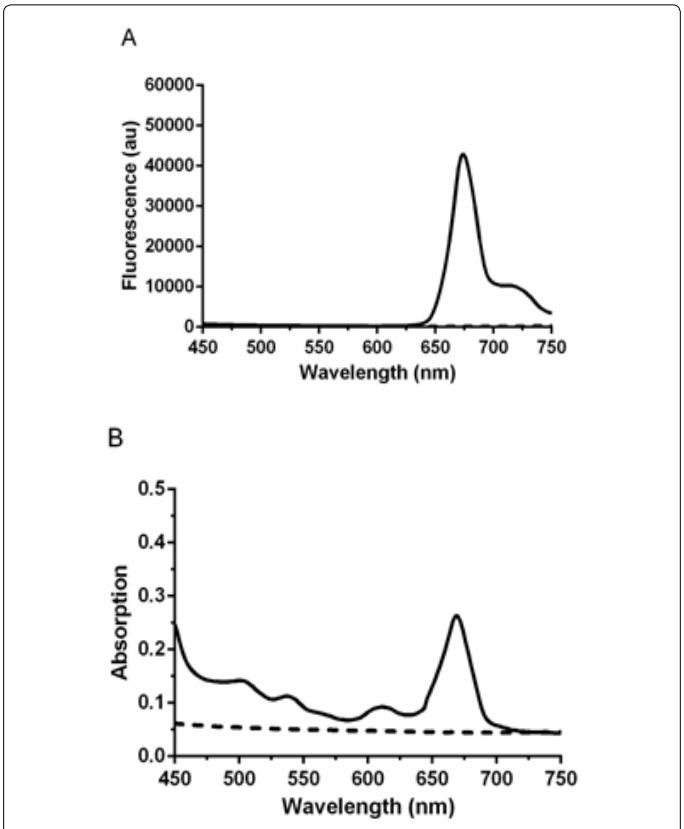

Figure 1: Fluorescence (A, excitation at λ 400 nm) and absorption (B) spectra of *Arrabidaea chica* extract nanoemulsion (ACE-NE, 140 µg ACE/mL, solid line) and blank nanoemulsion (BL-NE, discontinuous line).

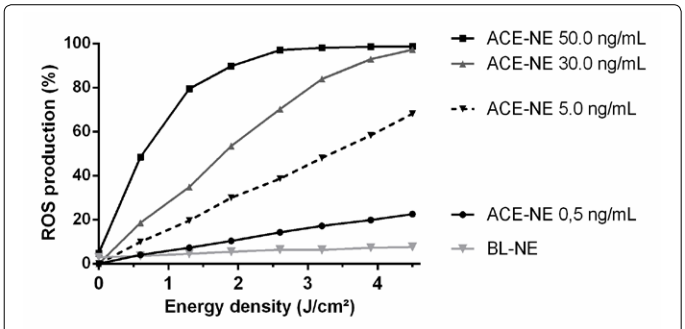

Figure 2: Production of reactive oxygen species (ROS) by *Arrabidaea chica* extract nanoemulsion (ACE-NE, different concentrations) and blank nanoemulsion (BL-NE) irradiated with different energy densities.

concentrations tested (Figure 3). When these cells were exposed to ACE-NE and irradiated, however, there was an ACE concentration-dependent reduction in their viability (CC_{50} = 4.8 µg/mL, CC100 = 20.0 µg/mL for MCF-10A; CC_{50} = 1.3 µg/mL, CC100 = 7.0 µg/mL for MCF-7).

PDT mediated by ACE-NE against spheroids of MCF-7 cells *in vitro*

Nor LED light alone neither ACE-NE alone was toxic to MCF-7 cells spheroids, as shown in Figure 4. When the spheroids were exposed for 30 or 60 minutes for ACE-NE and then irradiated, however, spheroid cells lysis was observed at all conditions tested. Irradiation of spheroids incubated with ACE-NE 60 µg ACE/mL for 30 minutes induced a 4.7-fold increase in LDH release in comparison to spheroids treated with ACE-NE at the same concentration and incubation time in the dark. Irradiation of spheroids incubated with ACE-NE 60 µg ACE/mL for 60 minutes, or incubation with ACE-NE 110 and 230 µg ACE/mL, for both 30 and 60 minutes, induced a 6-fold increase in LDH release in comparison to their respective controls in the dark.

Subcellular distribution of ACE-NE in MCF-7 cells

MCF-7 monolayer cells exposed for 15 minutes to ACE-NE presented intense fluorescence in their cytoplasm, as shown by Figure 5. Their nuclei were not stained by ACE-NE.

Discussion

Since the early 1980's, the development of new PS molecules has been a main line of research in PDT. Different molecules have been characterized for their photodynamic activity, but so far none present all the characteristics of an ideal PS. While some PS were obtained synthetically, several others were somehow derived from or inspired by nature [1,5,8,18]. In this context, if compared to other biomes, the Amazon ecosystem has been only poorly studied for the therapeutic potential of its species. This is also the case for the search of new PS molecules. In the present work, *A. chica* is presented as a potential source of new PS molecules.

ACE showed good photodynamic activity in the *in vitro* studies

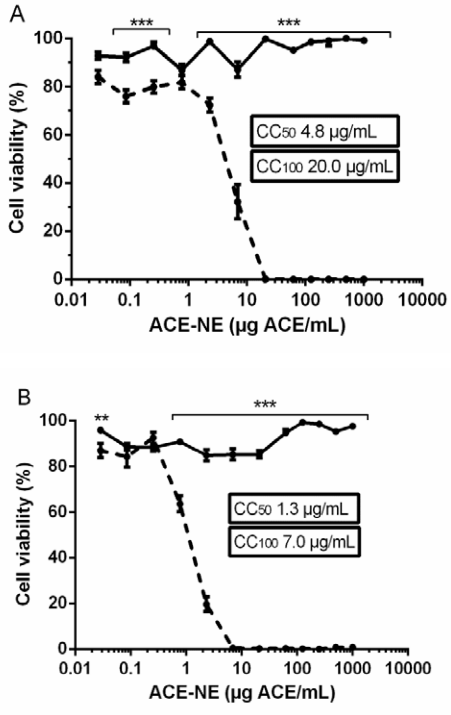

Figure 3: Viability of MCF-10A (A) and MCF-7 cells (B) exposed to different concentrations of *Arrabidaea chica* extract nanoemulsion (ACE-NE) for 15 minutes, and then kept in the dark (solid line) or irradiated (λ 660 nm, 4.5 J/cm², discontinuous line). Cells viability was evaluated by MTT method 24 hours after treatments. **p<0.01 for dark vs irradiated; ***p<0.001 for dark vs irradiated.

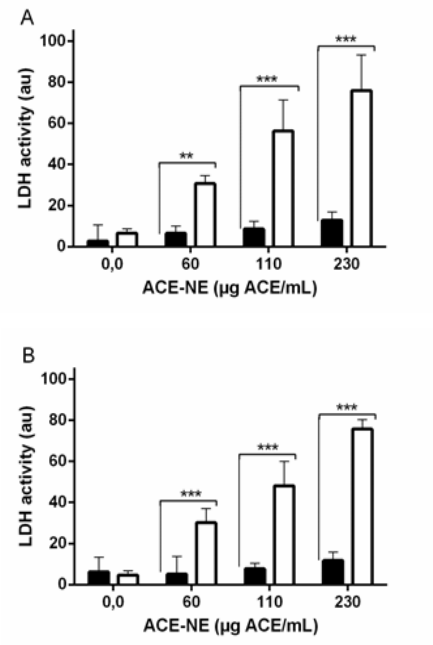

Figure 4: Lysis of MCF-7 spheroid cells expressed as arbitrary units (au) of lactate dehydrogenase (LDH) activity in the culture supernatant in arbitrary units (au). Spheroids were exposed to different concentrations of ACE-NE (expressed as µg of ACE/mL) for 30 minutes (A) or 60 minutes (B), and then kept in the dark (black columns) or irradiated (λ 660 nm, 4.5 J/cm², white columns). **p<0.01 and ***p<0.001 vs dark at the same ACE concentration.

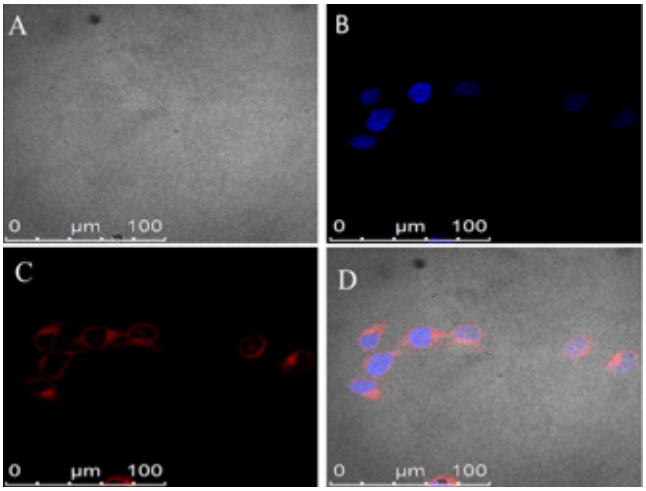

Figure 5: Subcellular distribution of ACE-NE (125 µg ACE/mL) by MCF-7 cells *in vitro* after 15 minutes of exposure. ACE appears in red, while nuclei are stained blue by 4',6-diamidino-2-phenylindole (DAPI). A) bright field. B) cells nuclei in blue. C) AlPc in red. D) merge of A, B and C.

presented in this work. This extract is hydrophobic, as it was obtained through sequential extraction with ethanol and chloroform. Hydrophobicity has been proved to be an advantageous characteristic of different PS molecules. For example, in comparison to hydrophilic derivatives, hydrophobic phthalocyanine derivatives, were shown to be more intensely accumulated by cancerous cells [19]. Therefore, this screening for PS molecules was focused on the hydrophobic molecules of *A. chica*. In order to perform tests in aqueous media, ACE was first nanoemulsified through a PIT method, giving a fine, transparent dispersion of nanodroplets ca 29 nm in diameter (ACE-NE).

In water, a peak of light absorption by ACE-NE was observed at the red region, specifically at 668 nm. This was the first characteristic presented by ACE suggesting it could be a source of PS molecules. For PDT, the optics of biological tissues and the energy necessary for the photodynamic processes to happen have to be taken into account. At first, biological tissues absorb light intensely between 400 and 600 nm, but poorly between 600 and 800 nm [4,11,20]. Therefore, PS absorbing light between 600 and 800 nm, the optical window of biological tissues, are more prone to be photoactivated at deeper layers of biological tissues. Secondly, wavelengths longer than 800 nm do not have energy enough for converting $^3O_2$ into $^1O_2$ [21], thus, 800 nm is the higher limit of light absorption for PS molecules – some upconversion systems have been designed for PDT with wavelengths longer than 800 nm [22]. Therefore, as ACE absorbed light in the region of interest for PDT, its ability to produce ROS under irradiation, a key event in PDT, was investigated.

ACE-NE, even in concentrations on the order of ng/mL, produced ROS when irradiated at a light density of 4.5 J/cm^2. This ROS production occurred in an aqueous medium, suggesting that the hydrophobic PS molecules in ACE were protected from quenching effects by the nanoemulsion oily phase. Generally, associating hydrophobic PS to drug carriers, mainly nanostructures, improves their photodynamic activity in aqueous media [4,7,9,23,24]. The photoactivated production of ROS by ACE-NE observed *in vitro* suggested it could present phototoxicity against cells *in vitro*. Thus, the subsequent experiments tested the *in vitro* cytotoxicity of PDT against human breast adenocarcinoma MCF-7 cells (spheroids and monolayers), and human mammary epithelial MCF-10A cells (monolayers). These cells were chosen in this study because: a) they are reported in several works with chemotherapeutics in the literature, b) breast cancer has a high incidence [25], and c) a PDT protocol is already under clinical trial for the treatment of breast cancer [6].

ACE-NE intensely reduced the viability of MCF-7 cells in the PDT protocol described in this work. Noteworthy, the CC_{50} of photoactivated ACE-NE against MCF-7 cells was 1.3 μg/mL, which can be considered acceptable for PDT, taken into account that the whole extract was used in this work. For means of comparison, the *in vitro* CC_{50} observed with the pure PS hypericin against MCF-7 cells was 1.84 μM, or 0.9 μg/mL [26]. ACE-NE was also effective in lysing MCF-7 cells organized in spheroids. In comparison to monolayers, cells spheroids closely mimic, *in vitro*, the architecture of solid tumors observed *in vivo* [16,27]. Spheroids are more resistant to treatments than cells in monolayers, since in spheroids the drug has to penetrate into the cell mass to induce its effect in deeper layers of cells [16]. Noteworthy, the increase in LDH release from MCF-7 cells spheroids treated with PDT based on ACE-NE ranged from 4.7-fold to 6.5-fold, which can be considered high if compared with previous results reported elsewhere [16]. Interestingly, at the concentration of 110 μg ACE/mL and 30 minutes of incubation, the maximum LDH release in comparison to the non-irradiated control was reached, with no further PDT-associated lysis observed at 60 minutes of incubation. It is thus probable that penetration of ACE-NE in MCF-7 spheroids was not more intense after 30 minutes of incubation.

Interestingly, the cytoplasm of MCF-7 cells was intensely stained by ACE after only 15 minutes of exposure to ACE-NE. This is correlated to the efficacy of PDT in these cells. Noteworthy, the fact that ACE was not found in significant amounts inside the MCF-7 cells nuclei is an advantageous characteristic of ACE-NE. PS accumulation inside the nucleus may induce genome damages that could potentially induce chemotherapeutic drugs-resistance in cancerous cells [5].

Non-cancerous cells were also susceptible to PDT mediated to ACE-NE. This is expected, since PDT elicits a strong oxidative burst [11], which is toxic not only to cancerous cells, but also to normal cells [7]. In PDT, adverse cytotoxic effects can be limited by focusing the activating light spot onto the tumor mass [6]. Finally, ACE-NE was not toxic in the dark to the tested cells, in all concentrations tested, which is an essential characteristic for PS [5,28].

Conclusions

This work shows that the hydrophobic extract from the aerial parts of *Arrabidaea chica* is a potential source of new PS molecules. Further investigations have to be focused on the purification and structure elucidation of PS molecules present in ACE, as well as on its *in vivo* activity in experimental cancer models.

Acknowledgements

Financial support from the Brazilian agencies National Institute of Science and Technology for Nanobiotechnology (MCT/CNPq), FINEP, CAPES, FAP/DF, and FINATEC is gratefully acknowledged.

Compliance with Ethical Standards

Disclosure of potential conflicts of interest. The authors declare that they have no conflict of interest.

References

1. Newman DJ, Cragg GM (2012) Natural products as sources of new drugs over the 30 years from 1981 to 2010. J Nat Prod 75: 311-335.
2. Vormisto J, Svenning JC, Hall P, Balslev H (2004) Diversity and dominance in palm (Arecaceae) communities in terra firme forests in the western Amazon basin. Journal of Ecology 92: 577-588.
3. Castano AP, Mroz P, Hamblin MR (2006) Photodynamic therapy and anti-tumour immunity. Nat Rev Cancer 6: 535-545.
4. Monge-Fuentes V, Muehlmann LA, de Azevedo R (2014) Perspectives on the application of nanotechnology in photodynamic therapy for the treatment of melanoma. Nano Rev 5.
5. Yano S, Hirohara S, Obata M, Hagiya Y, Ogura SI, et al. (2011) Current states and future views in photodynamic therapy. Journal of Photochemistry and Photobiology C: Photochemistry Reviews 12: 46-67.
6. Agostinis P, Berg K, Cengel KA, Foster TH, Girotti AW, et al. (2011) Photodynamic therapy of cancer: an update. CA Cancer J Clin 61: 250-281.
7. Muehlmann LA, Ma BC, Longo JPF, Santos MdFMA, Azevedo RB (2014) Aluminum–phthalocyanine chloride associated to poly (methyl vinyl ether-co-maleic anhydride) nanoparticles as a new third-generation photosensitizer for anticancer photodynamic therapy. International journal of nanomedicine 9: 1199.
8. Ormond AB, Freeman HS (2013) Dye sensitizers for photodynamic therapy. Materials 6: 817-840.
9. Muehlmann L, Joanitti G, Silva J, Longo J, Azevedo R (2011) Liposomal photosensitizers: potential platforms for anticancer photodynamic therapy. Brazilian Journal of Medical and Biological Research 44: 729-737.

10. Lovell JF, Liu TW, Chen J, Zheng G (2010) Activatable photosensitizers for imaging and therapy. Chem Rev 110: 2839-2857.

11. Dougherty TJ, Gomer CJ, Henderson BW, Jori G, Kessel D, et al. (1998) Photodynamic therapy. J Natl Cancer Inst 90: 889-905.

12. Zorn B, García-Piñeres AJ, Castro V, Murillo R, Mora G, et al. (2001) 3-Desoxyanthocyanidins from Arrabidaea chica. Phytochemistry 56: 831-835.

13. Anton N, Vandamme TF (2009) The universality of low-energy nano-emulsification. Int J Pharm 377: 142-147.

14. He X, Wu X, Wang K, Shi B, Hai L (2009) Methylene blue-encapsulated phosphonate-terminated silica nanoparticles for simultaneous in vivo imaging and photodynamic therapy. Biomaterials 30: 5601-5609.

15. Spiller W, Kliesch H, Woehrle D, Hackbarth S, Roeder B, et al. (1998) Singlet oxygen quantum yields of different photosensitizers in polar solvents and micellar solutions. Journal of Porphyrins and Phthalocyanines 2: 145-158.

16. Perche F, Torchilin VP (2012) Cancer cell spheroids as a model to evaluate chemotherapy protocols. Cancer Biol Ther 13: 1205-1213.

17. Mosmann T (1983) Rapid colorimetric assay for cellular growth and survival: application to proliferation and cytotoxicity assays. J Immunol Methods 65: 55-63.

18. Wainwright M (2008) Photodynamic therapy: the development of new photosensitisers. Anti-Cancer Agents in Medicinal Chemistry (Formerly Current Medicinal Chemistry-Anti-Cancer Agents) 8: 280-291.

19. Chan WS, Marshall JF, Svensen R, Bedwell J, Hart IR (1990) Effect of sulfonation on the cell and tissue distribution of the photosensitizer aluminum phthalocyanine. Cancer Res 50: 4533-4538.

20. Bonnett R (1995) Photosensitizers of the porphyrin and phthalocyanine series for photodynamic therapy. Chem Soc Rev 24: 19-33.

21. Celli JP, Spring BQ, Rizvi I, Evans CL, Samkoe KS, et al. (2010) Imaging and photodynamic therapy: mechanisms, monitoring, and optimization. Chem Rev 110: 2795-2838.

22. Idris NM, Gnanasammandhan MK, Zhang J, Ho PC, Mahendran R, et al. (2012) In vivo photodynamic therapy using upconversion nanoparticles as remote-controlled nanotransducers. Nature medicine 18: 1580-1585.

23. Lu HL, Syu WJ, Nishiyama N, Kataoka K, Lai PS (2011) Dendrimer phthalocyanine-encapsulated polymeric micelle-mediated photochemical internalization extends the efficacy of photodynamic therapy and overcomes drug-resistance in vivo. Journal of Controlled Release 155: 458-464.

24. Mijan M, Longo J, Melo L, Simioni A, Tedesco A (2014) Vascular Shutdown and Pro-inflammatory Cytokine Expression in Breast Cancer Tumors after Photodynamic Therapy Mediated by Nano-sized Liposomes Containing Aluminium-Chloride-Phthalocyanine. J Nanomed Nanotechnol 5: 2.

25. Siegel R, Ma J, Zou Z, Jemal A (2014) Cancer statistics, 2014. CA Cancer J Clin 64: 9-29.

26. Vandenbogaerde AL, Cuveele JF, Proot P, Himpens BE, Merlevede WJ, et al. (1997) Differential cytotoxic effects induced after photosensitization by hypericin. J Photochem Photobiol B 38: 136-142.

27. Desoize B, Jardillier J (2000) Multicellular resistance: a paradigm for clinical resistance? Crit Rev Oncol Hematol 36: 193-207.

28. Detty MR, Gibson SL, Wagner SJ (2004) Current clinical and preclinical photosensitizers for use in photodynamic therapy. J Med Chem 47: 3897-3915.